



KEK Preprint 2000-79  
BELLE-CONF-0008  
August 2000  
H

# Measurement of Inclusive Production of Neutral Pions from $\Upsilon(4S)$ Decays

The Belle Collaboration

*Submitted to the XXX<sup>th</sup> International Conference on High Energy Physics,  
July-August 2000, Osaka, Japan.*

**High Energy Accelerator Research Organization (KEK)**

KEK Reports are available from:

Information Resources Division  
High Energy Accelerator Research Organization (KEK)  
1-1 Oho, Tsukuba-shi  
Ibaraki-ken, 305-0801  
JAPAN

Phone: +81-298-64-5137

Fax: +81-298-64-4604

E-mail: [adm-jouhoushiryoku1@ccgemail.kek.jp](mailto:adm-jouhoushiryoku1@ccgemail.kek.jp)

Internet: <http://www.kek.jp>

## Measurement of Inclusive Production of Neutral Pions from $\Upsilon(4S)$ Decays

The Belle Collaboration

(Dated: July 16, 2000)

### Abstract

Using the Belle detector operating at the KEKB  $e^+e^-$  storage ring, we have measured the inclusive branching fraction<sup>a</sup> for  $\mathcal{B}(B \rightarrow \pi^0 X) = (251 \pm 5 \pm 16)\%$  and the momentum spectrum of neutral pions from the decays of the  $\Upsilon(4S)$  resonance. The results reported here are preliminary.

<sup>a</sup>Inclusive branching fractions have a definition in terms of multiplicity and can be greater than 100% [1].

A. Abashian<sup>44</sup>, K. Abe<sup>8</sup>, K. Abe<sup>36</sup>, I. Adachi<sup>8</sup>, Byoung Sup Ahn<sup>14</sup>, H. Aihara<sup>37</sup>, M. Akatsu<sup>19</sup>, G. Alimonti<sup>7</sup>, K. Aoki<sup>8</sup>, K. Asai<sup>20</sup>, M. Asai<sup>9</sup>, Y. Asano<sup>42</sup>, T. Aso<sup>41</sup>, V. Aulchenko<sup>2</sup>, T. Aushev<sup>12</sup>, A. M. Bakich<sup>33</sup>, E. Banas<sup>15</sup>, S. Behari<sup>8</sup>, P. K. Behera<sup>43</sup>, D. Beilene<sup>2</sup>, A. Bondar<sup>2</sup>, A. Bozek<sup>15</sup>, T. E. Browder<sup>7</sup>, B. C. K. Casey<sup>7</sup>, P. Chang<sup>23</sup>, Y. Chao<sup>23</sup>, B. G. Cheon<sup>32</sup>, S.-K. Choi<sup>6</sup>, Y. Choi<sup>32</sup>, Y. Doi<sup>8</sup>, J. Dragic<sup>17</sup>, A. Drutskoy<sup>12</sup>, S. Eidelman<sup>2</sup>, Y. Enari<sup>19</sup>, R. Enomoto<sup>8,10</sup>, C. W. Everton<sup>17</sup>, F. Fang<sup>7</sup>, H. Fujii<sup>8</sup>, K. Fujimoto<sup>19</sup>, Y. Fujita<sup>8</sup>, C. Fukunaga<sup>39</sup>, M. Fukushima<sup>10</sup>, A. Garmash<sup>2,8</sup>, A. Gordon<sup>17</sup>, K. Gotow<sup>44</sup>, H. Guler<sup>7</sup>, R. Guo<sup>21</sup>, J. Haba<sup>8</sup>, T. Haji<sup>4</sup>, H. Hamasaki<sup>8</sup>, K. Hanagaki<sup>29</sup>, F. Handa<sup>36</sup>, K. Hara<sup>27</sup>, T. Hara<sup>27</sup>, T. Haruyama<sup>8</sup>, N. C. Hastings<sup>17</sup>, K. Hayashi<sup>8</sup>, H. Hayashii<sup>20</sup>, M. Hazumi<sup>27</sup>, E. M. Heenan<sup>17</sup>, Y. Higashi<sup>8</sup>, Y. Higasino<sup>19</sup>, I. Higuchi<sup>36</sup>, T. Higuchi<sup>37</sup>, T. Hirai<sup>38</sup>, H. Hirano<sup>40</sup>, M. Hirose<sup>19</sup>, T. Hojo<sup>27</sup>, Y. Hoshi<sup>35</sup>, K. Hoshina<sup>40</sup>, W.-S. Hou<sup>23</sup>, S.-C. Hsu<sup>23</sup>, H.-C. Huang<sup>23</sup>, Y.-C. Huang<sup>21</sup>, S. Ichizawa<sup>38</sup>, Y. Igarashi<sup>8</sup>, T. Iijima<sup>8</sup>, H. Ikeda<sup>8</sup>, K. Ikeda<sup>20</sup>, K. Inami<sup>19</sup>, Y. Inoue<sup>26</sup>, A. Ishikawa<sup>19</sup>, R. Itoh<sup>8</sup>, G. Iwai<sup>25</sup>, M. Iwai<sup>8</sup>, H. Iwasaki<sup>8</sup>, Y. Iwasaki<sup>8</sup>, D. J. Jackson<sup>27</sup>, P. Jalocho<sup>15</sup>, H. K. Jang<sup>31</sup>, M. Jones<sup>7</sup>, R. Kagan<sup>12</sup>, H. Kakuno<sup>38</sup>, J. Kaneko<sup>38</sup>, J. H. Kang<sup>45</sup>, J. S. Kang<sup>14</sup>, P. Kapusta<sup>15</sup>, K. Kasami<sup>8</sup>, N. Katayama<sup>8</sup>, H. Kawai<sup>3</sup>, M. Kawai<sup>3</sup>, N. Kawamura<sup>1</sup>, T. Kawasaki<sup>25</sup>, H. Kichimi<sup>8</sup>, D. W. Kim<sup>32</sup>, Heejong Kim<sup>45</sup>, H. J. Kim<sup>45</sup>, Hyunwoo Kim<sup>14</sup>, S. K. Kim<sup>31</sup>, K. Kinoshita<sup>5</sup>, S. Kobayashi<sup>30</sup>, S. Koike<sup>8</sup>, Y. Kondo<sup>8</sup>, H. Konishi<sup>40</sup>, K. Korotushenko<sup>29</sup>, P. Krokovny<sup>2</sup>, R. Kulasiri<sup>5</sup>, S. Kumar<sup>28</sup>, T. Kuniya<sup>30</sup>, E. Kurihara<sup>3</sup>, A. Kuzmin<sup>2</sup>, Y.-J. Kwon<sup>45</sup>, M. H. Lee<sup>8</sup>, S. H. Lee<sup>31</sup>, C. Leonidopoulos<sup>29</sup>, H.-B. Li<sup>11</sup>, R.-S. Lu<sup>23</sup>, Y. Makida<sup>8</sup>, A. Manabe<sup>8</sup>, D. Marlow<sup>29</sup>, T. Matsubara<sup>37</sup>, T. Matsuda<sup>8</sup>, S. Matsui<sup>19</sup>, S. Matsumoto<sup>4</sup>, T. Matsumoto<sup>19</sup>, K. Misono<sup>19</sup>, K. Miyabayashi<sup>20</sup>, H. Miyake<sup>27</sup>, H. Miyata<sup>25</sup>, L. C. Moffitt<sup>17</sup>, G. R. Moloney<sup>17</sup>, G. F. Moorhead<sup>17</sup>, N. Morgan<sup>44</sup>, S. Mori<sup>42</sup>, T. Mori<sup>4</sup>, A. Murakami<sup>30</sup>, T. Nagamine<sup>36</sup>, Y. Nagasaka<sup>18</sup>, Y. Nagashima<sup>27</sup>, T. Nakadaira<sup>37</sup>, T. Nakamura<sup>38</sup>, E. Nakano<sup>26</sup>, M. Nakao<sup>8</sup>, H. Nakazawa<sup>4</sup>, J. W. Nam<sup>32</sup>, S. Narita<sup>36</sup>, Z. Natkaniec<sup>15</sup>, K. Neichi<sup>35</sup>, S. Nishida<sup>16</sup>, O. Nitoh<sup>40</sup>, S. Noguchi<sup>20</sup>, T. Nozaki<sup>8</sup>, S. Ogawa<sup>34</sup>, R. Ohkubo<sup>8</sup>, T. Ohshima<sup>19</sup>, Y. Ohshima<sup>38</sup>, T. Okabe<sup>19</sup>, T. Okazaki<sup>20</sup>, S. Okuno<sup>13</sup>, S. L. Olsen<sup>7</sup>, W. Ostrowicz<sup>15</sup>, H. Ozaki<sup>8</sup>, P. Pakhlov<sup>12</sup>, H. Palka<sup>15</sup>, C. S. Park<sup>31</sup>, C. W. Park<sup>14</sup>, H. Park<sup>14</sup>, L. S. Peak<sup>33</sup>, M. Peters<sup>7</sup>, L. E. Pilonen<sup>44</sup>, E. Prebys<sup>29</sup>, J. Raaf<sup>6</sup>, J. L. Rodriguez<sup>7</sup>, N. Root<sup>2</sup>, M. Rozanska<sup>15</sup>, K. Rybicki<sup>15</sup>, J. Ryuko<sup>27</sup>, H. Sagawa<sup>8</sup>, Y. Sakai<sup>8</sup>, H. Sakamoto<sup>16</sup>, H. Sakaue<sup>26</sup>, M. Satapathy<sup>43</sup>, N. Sato<sup>8</sup>, A. Satpathy<sup>8,5</sup>, S. Schrenk<sup>44</sup>, S. Semenov<sup>12</sup>, Y. Settai<sup>4</sup>, M. E. Sevier<sup>17</sup>, H. Shibuya<sup>34</sup>, B. Shwartz<sup>2</sup>, A. Sidorov<sup>2</sup>, V. Sidorov<sup>2</sup>, S. Stanić<sup>42</sup>, A. Sugi<sup>19</sup>, A. Sugiyama<sup>19</sup>, K. Sumisawa<sup>27</sup>, T. Sumiyoshi<sup>8</sup>, J. Suzuki<sup>8</sup>, J.-I. Suzuki<sup>8</sup>, K. Suzuki<sup>3</sup>, S. Suzuki<sup>19</sup>, S. Y. Suzuki<sup>8</sup>, S. K. Swain<sup>7</sup>, H. Tajima<sup>37</sup>, T. Takahashi<sup>26</sup>, F. Takasaki<sup>8</sup>, M. Takita<sup>27</sup>, K. Tamai<sup>8</sup>, N. Tamura<sup>25</sup>, J. Tanaka<sup>37</sup>, M. Tanaka<sup>8</sup>, Y. Tanaka<sup>18</sup>, G. N. Taylor<sup>17</sup>, Y. Teramoto<sup>26</sup>, M. Tomoto<sup>19</sup>, T. Tomura<sup>37</sup>, S. N. Tovey<sup>17</sup>, K. Trabelsi<sup>7</sup>, T. Tsuboyama<sup>8</sup>, Y. Tsujita<sup>42</sup>, T. Tsukamoto<sup>8</sup>, T. Tsukamoto<sup>30</sup>, S. Uehara<sup>8</sup>, K. Ueno<sup>23</sup>, N. Ujii<sup>8</sup>, Y. Unno<sup>3</sup>, S. Uno<sup>8</sup>, Y. Ushiroda<sup>16</sup>, Y. Usov<sup>2</sup>, S. E. Vahsen<sup>29</sup>, G. Varner<sup>7</sup>, K. E. Varvell<sup>33</sup>, C. C. Wang<sup>23</sup>, C. H. Wang<sup>22</sup>, M.-Z. Wang<sup>23</sup>, T.-J. Wang<sup>11</sup>, Y. Watanabe<sup>36</sup>, E. Won<sup>31</sup>, B. D. Yabsley<sup>8</sup>, Y. Yamada<sup>8</sup>, M. Yamaga<sup>36</sup>, A. Yamaguchi<sup>36</sup>, H. Yamaguchi<sup>8</sup>, H. Yamamoto<sup>7</sup>, H. Yamaoka<sup>8</sup>, Y. Yamaoka<sup>8</sup>, Y. Yamashita<sup>24</sup>, M. Yamauchi<sup>8</sup>, S. Yanaka<sup>38</sup>, M. Yokoyama<sup>37</sup>, K. Yoshida<sup>19</sup>, Y. Yusa<sup>36</sup>, H. Yuta<sup>1</sup>, C.-C. Zhang<sup>11</sup>, H. W. Zhao<sup>8</sup>, Y. Zheng<sup>7</sup>, V. Zhilich<sup>2</sup>, and D. Zontar<sup>42</sup>

<sup>1</sup>Aomori University, Aomori

<sup>2</sup>Budker Institute of Nuclear Physics, Novosibirsk

<sup>3</sup>Chiba University, Chiba

- <sup>4</sup>Chuo University, Tokyo  
<sup>5</sup>University of Cincinnati, Cincinnati, OH  
<sup>6</sup>Gyeongsang National University, Chinju  
<sup>7</sup>University of Hawaii, Honolulu HI  
<sup>8</sup>High Energy Accelerator Research Organization (KEK), Tsukuba  
<sup>9</sup>Hiroshima Institute of Technology, Hiroshima  
<sup>10</sup>Institute for Cosmic Ray Research, University of Tokyo, Tokyo  
<sup>11</sup>Institute of High Energy Physics, Chinese Academy of Sciences, Beijing  
<sup>12</sup>Institute for Theoretical and Experimental Physics, Moscow  
<sup>13</sup>Kanagawa University, Yokohama  
<sup>14</sup>Korea University, Seoul  
<sup>15</sup>H. Niewodniczanski Institute of Nuclear Physics, Krakow  
<sup>16</sup>Kyoto University, Kyoto  
<sup>17</sup>University of Melbourne, Victoria  
<sup>18</sup>Nagasaki Institute of Applied Science, Nagasaki  
<sup>19</sup>Nagoya University, Nagoya  
<sup>20</sup>Nara Women's University, Nara  
<sup>21</sup>National Kaohsiung Normal University, Kaohsiung  
<sup>22</sup>National Lien-Ho Institute of Technology, Miao Li  
<sup>23</sup>National Taiwan University, Taipei  
<sup>24</sup>Nihon Dental College, Niigata  
<sup>25</sup>Niigata University, Niigata  
<sup>26</sup>Osaka City University, Osaka  
<sup>27</sup>Osaka University, Osaka  
<sup>28</sup>Panjab University, Chandigarh  
<sup>29</sup>Princeton University, Princeton NJ  
<sup>30</sup>Saga University, Saga  
<sup>31</sup>Seoul National University, Seoul  
<sup>32</sup>Sungkyunkwan University, Suwon  
<sup>33</sup>University of Sydney, Sydney NSW  
<sup>34</sup>Toho University, Funabashi  
<sup>35</sup>Tohoku Gakuin University, Tagajo  
<sup>36</sup>Tohoku University, Sendai  
<sup>37</sup>University of Tokyo, Tokyo  
<sup>38</sup>Tokyo Institute of Technology, Tokyo  
<sup>39</sup>Tokyo Metropolitan University, Tokyo  
<sup>40</sup>Tokyo University of Agriculture and Technology, Tokyo  
<sup>41</sup>Toyama National College of Maritime Technology, Toyama  
<sup>42</sup>University of Tsukuba, Tsukuba  
<sup>43</sup>Utkal University, Bhubaneswer  
<sup>44</sup>Virginia Polytechnic Institute and State University, Blacksburg VA  
<sup>45</sup>Yonsei University, Seoul

This analysis presents the first results on the average multiplicity of neutral pions and their momentum spectrum in  $B$  meson decays at the  $\Upsilon(4S)$  resonance using the Belle detector [2] at KEKB [3]. The measurement is based on a large number of hadronic events collected by the Belle detector at a center-of-mass energy of  $\sqrt{s}=10.58$  GeV since June of 1999.

The particle composition of hadronic final states in  $e^+e^-$  annihilation and the measurement of inclusive particle production rates have been important subjects for various energy regions. Previous studies of particle composition at the  $\Upsilon(4S)$  resonance include measurements of charged particles ( $\pi^\pm$  [4, 5] and  $K^\pm$  [6, 7]) and  $\eta$  mesons [8], and other vector mesons [9, 10]. For typical  $B$  meson decays, the major part of neutral energy is carried by neutral pions while most studies of hadron production in the  $B$  decays in the  $\Upsilon(4S)$  energy have concentrated on charged particles. Measurements of inclusive neutral pion production are needed to improve Monte Carlo generators and to constrain unmeasured or poorly measured branching fractions.

The Belle detector, described in detail in Ref. [2], consists of a silicon vertex detector (SVD) [11], central drift chamber (CDC) [12], aerogel Cherenkov counter (ACC) [13], time of flight/trigger scintillation counter (TOF/TSC) [14], CsI electromagnetic calorimeter (ECL) [15] and  $K_L$ /muon detector (KLM) [16]. The SVD measures the precise position of decay vertices. It consists of three layers of double-sided silicon strip detectors (DSSD) in a barrel-only design and covers 86% of solid angle. The radius of each layer is 3.0, 4.5, and 6cm. Charged tracks are reconstructed primarily by the CDC, that covers the  $17^\circ < \theta < 150^\circ$  polar angular region. It consists of 50 cylindrical layers of drift cells organized into 11 super-layers (axial or small-angle-stereo) each containing between three and six layers. A He-C<sub>2</sub>H<sub>6</sub> (50/50%) gas is used to minimize multiple-Coulomb scattering. The inner and outer radii of the CDC are 9 cm and 86 cm, respectively. The magnetic field of 1.5 Tesla is chosen to optimize momentum resolution without sacrificing reconstruction efficiency for low momentum tracks. Kaon identification (KID) is provided by specific ionization ( $dE/dx$ ) measurements in the CDC, Cherenkov threshold measurements in the ACC, and the cylindrical TOF scintillator barrel. The ECL is made of finely segmented CsI(Tl) crystals 30 cm in length. The cross section of one counter is approximately  $55 \times 55 \text{mm}^2$  at the front surface. The ECL crystals cover the  $12^\circ < \theta < 157^\circ$  angular region. The inner radius of the barrel is 1.25m, while the annular endcaps are placed at +2.0m and -1.0m along the beam line from a beam-beam interaction point. The calibration of the calorimeter was performed by using cosmic rays and Bhabha events. The KLM consists of alternating layers of charged particle detectors and 4.7cm thick iron plates.

The data samples used in this analysis correspond to  $1.8 \text{ fb}^{-1}$  of integrated luminosity taken at the  $\Upsilon(4S)$  resonance and  $122 \text{ pb}^{-1}$  taken at a cms energy 60 MeV below the resonance; the latter was used to subtract underlying continuum background. The integrated luminosity was determined from the number of large-angle Bhabha events.

Hadronic events are selected based on event multiplicity and visible energy. The primary cuts are that an event must have at least three charged tracks with  $p_t > 100 \text{MeV}/c$  that originate near the interaction point and the sum of the energy of charged tracks and reconstructed photons ( $E_{\text{vis}}$ ) must be greater than 20% of  $\sqrt{s}$ . These two cuts remove the majority of beam gas/wall and two-photon backgrounds. Beam gas background is further reduced by cutting on the primary event vertex. Backgrounds from radiative Bhabha and higher multiplicity QED processes are suppressed by requiring the multiplicity of large-angle charged tracks and ECL clusters to be greater than 1, requiring the average cluster energy

to be below 1 GeV, and the total ECL cluster energy to be below 80% of  $\sqrt{s}$ . Tau pair events are identified and removed by reconstructing the invariant mass of particles found in hemispheres perpendicular to the event thrust axis and cutting out the tau peak. To regain hadronic events under the tau peak, we allow events to pass this cut if the invariant mass discussed above is greater than 25% of the visible energy. The selection is 99% efficient for  $B\bar{B}$  events, approximately 87% efficient for continuum events and contains a non hadronic contamination that varies from 2 to 5% due to the variations in beam background caused by the on going commissioning of KEKB. To suppress continuum, we required that the ratio of second to zeroth Fox-Wolfram moments  $R_2$  [17], determined using charged tracks and neutral clusters, be less than 0.5. The efficiency for the hadronic event selection was found by a Monte Carlo simulation program.

Photons are reconstructed from neutral clusters in the ECL that have a lateral shape consistent with that of an electromagnetic shower. Photon energy resolution was measured to be  $\sigma_E/E(\%) = 0.066/E \oplus 0.81/E^{0.25} \oplus 1.34$  ( $E$  in GeV) from beam tests [15]. To keep the combinatorial background at a reasonable level, only photons in the central barrel region ( $35^\circ < \theta < 120^\circ$ ) with  $E_\gamma \geq 30$  MeV are used in this analysis; the endcap regions have worse energy resolution due to more intervening material and higher beam-associated background.

For each 100 MeV/c momentum bin in the cms momentum range 0 to 3 GeV/c, the  $\gamma\gamma$  invariant mass distribution was fit to an asymmetric (symmetric above 2 GeV/c) Gaussian for the signal plus a polynomial for the combinatorial background to extract the  $\pi^0$  yields in each momentum interval. Figure 1 shows typical mass spectra obtained from the on-resonance data. For the asymmetric Gaussians, the mass resolution was defined as the mean of the left- and right-hand sigmas. An average mass resolution of 4.9 MeV/c<sup>2</sup> was obtained, dominated by energy resolution at low momenta or by angular resolution at high momenta. The mass peak is shifted slightly from the PDG value [1] because of the asymmetric energy response due to shower leakage. The observed mass peak and resolution are consistent with Monte Carlo expectations, as shown in Fig. 2. To extract the  $\pi^0$  spectrum from  $\Upsilon(4S)$  decays, the underlying continuum in the on-resonance data is subtracted bin-by-bin using off-resonance data taken at a cms energy 60 MeV below the resonance. The inclusive spectrum is calculated by :

$$\frac{1}{\sigma_h} \cdot \frac{d\sigma_{\pi^0}}{dp_{\pi^0}^*} = \frac{1}{N_h} \cdot \frac{Y_{on}^i - \alpha \cdot Y_{off}^i}{\epsilon^i \cdot \Delta p_{\pi^0}^*}, \quad (1)$$

where  $N_h$  is the number of  $B\bar{B}$  events corrected for event selection efficiency,  $\alpha = (L_{on}/L_{off}) \cdot (s_{off}/s_{on})$  is on-off scaling factor,  $Y_{on}$  and  $Y_{off}$  are background-subtracted  $\pi^0$  yields obtained from on- and off-resonance data fits, and  $\epsilon$  is the acceptance and detection efficiency factor for each momentum bin. To take the on-off cms energy difference into account, the off-resonance  $\pi^0$  momenta have been scaled by  $\sqrt{s_{on}/s_{off}}$ . The average  $\pi^0$  multiplicity was obtained by integrating the measured momentum spectrum as shown in Table I.

Possible sources of systematic uncertainties and their effect on the inclusive  $\pi^0$  mean multiplicity measurement are summarized in Table II. The uncertainties in the number of  $B\bar{B}$  events and the hadronic event selection efficiency were estimated to be 1% and 1.3%, respectively, or 1.6% combined. The uncertainty in the relative luminosity ratio, used to subtract the continuum background from the on-resonance data, contributes a 2% variation in our  $\pi^0$  mean multiplicity measurement. The assumption that the momenta scale with cms energy in applying the continuum subtraction has a 0.8% uncertainty (determined by ignoring this scaling during the subtraction). The uncertainty in the  $\pi^0$  detection efficiency

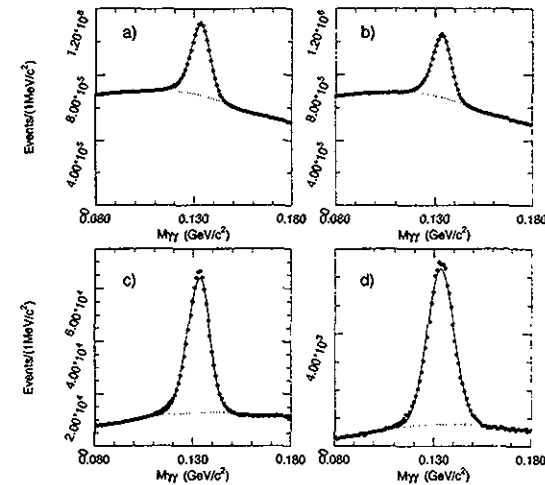


FIG. 1:  $\gamma\gamma$  invariant mass distributions for the  $\Upsilon(4S)$  resonance data. (a)  $P_{\gamma\gamma}^*$  0.0-3.0 GeV/c; (b) 0.0-1.0 GeV/c; (c) 1.0-2.0 GeV/c; (d) 2.0-3.0 GeV/c. An average mass resolution of 4.9 MeV/c<sup>2</sup> was obtained. The smooth curve in the plots is a fit to the data using an asymmetric (or symmetric) Gaussian plus a polynomial.

due to the application of the shower transverse shape cut, the charged-track veto, and the ECL's modest non-linear energy response correction are estimated to be 0.4%, 1.6%, and 0.6%, respectively (determined by comparing the yields with and without each of these criteria).

The  $\pi^0$  acceptance and detection efficiency are determined from Monte Carlo simulations of  $B\bar{B}$  decays (equal proportions of charged and neutral  $B$  mesons) and continuum processes. The  $\gamma\gamma$  invariant mass distributions are fit with the same functions as used in the real data analysis. The product of acceptance and detection efficiency are defined as the ratio of the fitted  $\pi^0$  yield to the generated count. Efficiencies for the high momentum  $\pi^0$ 's above the kinematic limit for  $B\bar{B}$  decays are deduced from continuum Monte Carlo normalized at 2.2-2.3 GeV/c bin and scaled efficiencies are used that accounts for different acceptance.

The decay angular distribution for the photons in the  $\pi^0$  rest frame is expected to be isotropic, but the detected distribution of the decay angle  $\theta_d$ — defined as the angle between the photon momentum in the  $\pi^0$  rest frame and  $\pi^0$  momentum in any reference frame— shows energy dependence due to the  $\gamma$  energy cut. This can be used to suppress random combinatorial backgrounds. Furthermore, a disagreement between the photon detection efficiency between Monte Carlo and data would manifest itself as a discrepancy in the decay angular distribution, which can, therefore, be used to estimate the uncertainty in the  $\pi^0$

Belle Preliminary

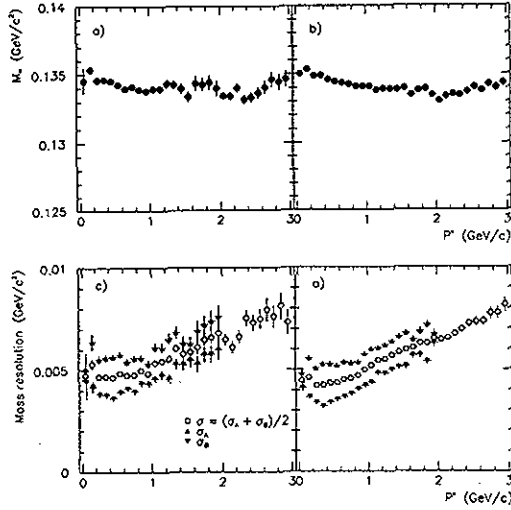


FIG. 2: Mass resolution and peak obtained from off-resonance data and Monte Carlo expectations. (a),(c) data; (b),(d) continuum Monte Carlo. The fluctuations around 2 GeV/c were caused by changing the signal fitting function from an asymmetric to a symmetric Gaussian.

detection efficiency. A comparison of the decay angular distributions between Monte Carlo and data for  $|\cos\theta_d| > 0.5$  and  $|\cos\theta_d| \leq 0.5$  leads to a 0.3% uncertainty in the  $\pi^0$  detection efficiency.

The  $\gamma\gamma$  invariant mass distribution for each momentum bin is fit to the following functions in the mass window 80 - 180 MeV/c<sup>2</sup>:

- $P_{\gamma\gamma}^* < 1.0$  GeV/c: 4th order polynomial plus bifurcated Gaussian.
- $1.0 \leq P_{\gamma\gamma}^* < 2.0$  GeV/c: 2nd order polynomial plus bifurcated Gaussian.
- $2.0 \leq P_{\gamma\gamma}^* < 3.0$  GeV/c: 2nd order polynomial plus Gaussian.

The fitting range and the order of the polynomial are chosen to minimize statistical fluctuation. By changing the order of polynomial from 2 to 4, the relative yield variation between data and Monte Carlo,  $R = (Y_{data}^{4th}/Y_{data}^{2nd})/(Y_{mc}^{4th}/Y_{mc}^{2nd})$ , is taken as the systematic uncertainty in the background modeling, a 2.8% uncertainty was assigned. The weighted average of fit errors in the efficiency estimation,  $(\delta\epsilon)^2 = \sum_i \sigma_{i,i}^2 \cdot Y_i^{\pi^0} / \sum_i Y_i^{\pi^0}$ , leads to 1.2% uncertainty. Combining these two numbers gives a 3% systematic uncertainty in the  $\pi^0$  mean multiplicity measurement due to the fit procedure.

To estimate the run- and data-set dependence of the  $\pi^0$  spectrum measurement, the analysis was repeated for several subsets of on-resonance data sample taken just before and

Belle Preliminary

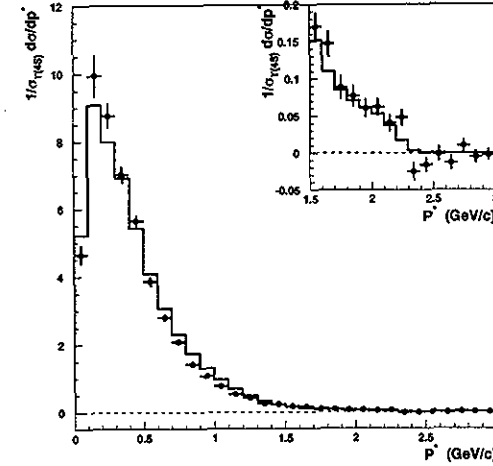


FIG. 3: Measured inclusive  $\pi^0$  spectrum in the  $\Upsilon(4S)$  decays, the histogram shows Monte Carlo prediction. Only statistical errors are shown. Fluctuations in the 2.2-2.4 GeV/c bins are from the off-resonance data.

after the off-resonance data taking. The largest deviation (4.6%) among these subsets was taken as the systematic uncertainty from run dependence, assuming that this deviation was real.

The measured  $\pi^0$  spectrum is compared to the  $B\bar{B}$  Monte Carlo [18] prediction in Fig. 3. Systematic differences in the intermediate momentum region may be caused by overestimated  $b \rightarrow c$  processes in the Monte Carlo event generation; these could bias our acceptance and detection efficiency. However, the average multiplicity differed between data and Monte Carlo by less than 1%—small compared to the statistical and other systematic uncertainties. In the high momentum region, no significant excess is observed; however, here the statistical precision is limited and the fluctuations are dominated by the off-resonance data used in the subtraction. Additional data are needed for this comparison.

In conclusion, using 1.8 fb<sup>-1</sup> of data accumulated at the  $\Upsilon(4S)$  resonance by the Belle detector, we have measured the inclusive spectrum of neutral pions from  $\Upsilon(4S)$  decays. By integrating over the measured momentum bins, the mean multiplicity of neutral pions from  $\Upsilon(4S)$  decays has been determined to be  $\langle n_{\pi^0} \rangle = 5.01 \pm 0.09 \pm 0.32$ , corresponding to an inclusive branching fraction of  $B(B \rightarrow \pi^0 X) = (251 \pm 5 \pm 16)\%$ , where the first error is statistical and the second is systematic. The results reported here are preliminary.

## ACKNOWLEDGMENTS

We gratefully acknowledge the efforts of the KEKB group in providing us with excellent luminosity and running conditions and the help with our computing and network systems provided by members of the KEK computing research center. We thank the staffs of KEK and collaborating institutions for their contributions to this work, and acknowledge support from the Ministry of Education, Science, Sports and Culture of Japan and the Japan Society for the Promotion of Science; the Australian Research Council and the Australian Department of Industry, Science and Resources; the Department of Science and Technology of India; the BK21 program of the Ministry of Education of Korea and the Basic Science program of the Korea Science and Engineering Foundation; the Polish State Committee for Scientific Research under contract No.2P03B 17017; the Ministry of Science and Technology of Russian Federation; the National Science Council and the Ministry of Education of Taiwan; the Japan-Taiwan Cooperative Program of the Interchange Association; and the U.S. Department of Energy.

## REFERENCES

- [1] Particle Data Group: C. Caso *et al.*, Eur. Phys. J. **C3**, 1 (1998).
- [2] Belle Technical Design Report, KEK Report 95-1, April 1995.
- [3] KEKB B-Factory Design Report, KEK Report 95-7, August 1995.
- [4] CLEO Collaboration, M. S. Alam *et al.*, Phys. Rev. Lett. **49**, 357 (1982).
- [5] ARGUS Collaboration, H. Albrecht *et al.*, Z. Phys. **C58**, 191 (1993).
- [6] CLEO Collaboration, M. S. Alam *et al.*, Phys. Rev. Lett. **58**, 1814 (1987).
- [7] ARGUS Collaboration, H. Albrecht *et al.*, Z. Phys. **C62**, 371 (1994).
- [8] CLEO Collaboration, Y. Kubota *et al.*, Phys. Rev. **D53**, 6033 (1996).
- [9] CLEO Collaboration, D. Bortoletto *et al.*, Phys. Rev. Lett. **56**, 800 (1986).
- [10] ARGUS Collaboration, H. Albrecht *et al.*, Z. Phys. **C61**, 1 (1994).
- [11] G. Alimonti *et al.*, "The Belle silicon vertex detector," KEK preprint 2000-34.
- [12] H. Hirano *et al.*, KEK Preprint 2000-2. M. Akatsu *et al.*, DPNU-00-06.
- [13] T. Iijima *et al.*, "Aerogel Cherenkov counter for the Belle detector," Proceedings of the 7th International Conference on Instrumentation for Colliding Beam Physics, Hamamatsu, Japan, Nov. 15-19, 1999.
- [14] H. Kichimi *et al.*, "The Belle TOF system," Proceedings of the 7th International Conference on Instrumentation for Colliding Beam Physics, Hamamatsu, Japan, Nov. 15-19, 1999.
- [15] H. Ikeda *et al.*, Nucl. Instrum. and Meth. **A441**, 401 (2000).
- [16] A. Abashian *et al.*, Nucl. Instrum. and Meth. **A449**, 112 (2000).
- [17] G. Fox and S. Wolfram, Phys. Rev. Lett. **41**, 1581 (1978).
- [18] QQ Monte Carlo event generator developed by the CLEO Experiment.

TABLE I: Measured inclusive  $\pi^0$  spectrum from  $\Upsilon(4S)$  decays, using  $1.8 \text{ fb}^{-1}$  on-resonance and  $122 \text{ pb}^{-1}$  off-resonance data (results are preliminary). Errors are statistical only.

$P^*$ (GeV/c)	$Y_{on}$	$Y_{off}$	$Y_{on} - \alpha Y_{off}$	$\epsilon$ (%)	$\frac{1}{\sigma_s} \frac{d\sigma}{dp^*}$
0.0-0.1	241947.0 $\pm$ 3693.6	5199.2 $\pm$ 617.5	166242.2 $\pm$ 9721.1	19.1	4.656 $\pm$ 0.272
0.1-0.2	626226.0 $\pm$ 5991.2	23159.0 $\pm$ 1169.3	289011.3 $\pm$ 18049.4	15.5	9.936 $\pm$ 0.621
0.2-0.3	661225.0 $\pm$ 3994.5	27137.0 $\pm$ 726.4	266087.2 $\pm$ 11305.5	16.2	8.760 $\pm$ 0.372
0.3-0.4	692758.0 $\pm$ 3043.5	29748.0 $\pm$ 592.4	259601.8 $\pm$ 9147.6	19.8	7.015 $\pm$ 0.247
0.4-0.5	618697.0 $\pm$ 2372.1	26191.0 $\pm$ 467.0	237333.8 $\pm$ 7201.6	22.5	5.640 $\pm$ 0.171
0.5-0.6	512643.0 $\pm$ 1887.9	22936.0 $\pm$ 410.2	178675.3 $\pm$ 6264.0	24.7	3.861 $\pm$ 0.135
0.6-0.7	410696.0 $\pm$ 1575.8	18624.0 $\pm$ 329.4	139514.7 $\pm$ 5047.9	26.6	2.802 $\pm$ 0.101
0.7-0.8	325629.0 $\pm$ 1322.7	14870.0 $\pm$ 273.6	109109.2 $\pm$ 4198.2	27.9	2.087 $\pm$ 0.080
0.8-0.9	252751.0 $\pm$ 1104.6	12022.0 $\pm$ 242.1	77700.4 $\pm$ 3693.6	29.2	1.421 $\pm$ 0.068
0.9-1.0	198119.0 $\pm$ 951.1	9412.4 $\pm$ 200.9	61066.4 $\pm$ 3075.7	30.2	1.079 $\pm$ 0.054
1.0-1.1	163716.0 $\pm$ 674.5	8051.6 $\pm$ 150.5	46477.9 $\pm$ 2292.4	32.4	0.766 $\pm$ 0.038
1.1-1.2	128108.0 $\pm$ 586.2	6539.8 $\pm$ 134.3	32882.9 $\pm$ 2041.4	33.2	0.528 $\pm$ 0.033
1.2-1.3	102437.0 $\pm$ 514.8	5199.4 $\pm$ 118.0	26729.3 $\pm$ 1793.4	33.6	0.425 $\pm$ 0.029
1.3-1.4	81448.0 $\pm$ 449.2	4512.4 $\pm$ 110.6	15743.6 $\pm$ 1671.4	33.8	0.249 $\pm$ 0.026
1.4-1.5	66284.0 $\pm$ 405.4	3562.0 $\pm$ 94.0	14418.2 $\pm$ 1427.8	33.7	0.228 $\pm$ 0.023
1.5-1.6	53339.0 $\pm$ 356.7	2903.1 $\pm$ 84.6	11067.4 $\pm$ 1282.6	34.8	0.170 $\pm$ 0.020
1.6-1.7	44009.0 $\pm$ 324.0	2340.1 $\pm$ 77.7	9935.2 $\pm$ 1176.5	36.0	0.147 $\pm$ 0.017
1.7-1.8	37283.0 $\pm$ 295.6	2151.8 $\pm$ 71.4	5951.0 $\pm$ 1080.8	35.9	0.089 $\pm$ 0.016
1.8-1.9	30914.0 $\pm$ 263.8	1763.2 $\pm$ 63.4	5240.3 $\pm$ 960.1	36.2	0.077 $\pm$ 0.014
1.9-2.0	25904.0 $\pm$ 236.3	1477.6 $\pm$ 59.1	4388.9 $\pm$ 892.3	38.5	0.061 $\pm$ 0.012
2.0-2.1	21145.0 $\pm$ 211.2	1164.0 $\pm$ 50.7	4196.2 $\pm$ 767.2	36.0	0.062 $\pm$ 0.011
2.1-2.2	16624.0 $\pm$ 187.5	975.3 $\pm$ 45.7	2423.4 $\pm$ 691.3	31.5	0.041 $\pm$ 0.012
2.2-2.3	13524.0 $\pm$ 168.9	744.0 $\pm$ 40.7	2691.2 $\pm$ 616.6	29.9	0.048 $\pm$ 0.011
2.3-2.4	10483.0 $\pm$ 150.4	814.6 $\pm$ 43.9	-1378.3 $\pm$ 657.1	29.4	-0.025 $\pm$ 0.012
2.4-2.5	8652.8 $\pm$ 135.0	655.7 $\pm$ 36.6	-894.3 $\pm$ 550.0	29.5	-0.016 $\pm$ 0.010
2.5-2.6	7412.3 $\pm$ 125.3	512.5 $\pm$ 34.4	-49.8 $\pm$ 515.9	26.8	-0.001 $\pm$ 0.010
2.6-2.7	5838.0 $\pm$ 113.2	445.0 $\pm$ 31.9	-641.0 $\pm$ 478.7	26.2	-0.013 $\pm$ 0.010
2.7-2.8	5091.6 $\pm$ 104.0	318.0 $\pm$ 26.7	461.5 $\pm$ 403.0	24.8	0.010 $\pm$ 0.009
2.8-2.9	4068.2 $\pm$ 95.6	294.8 $\pm$ 25.0	-224.2 $\pm$ 376.3	24.1	-0.005 $\pm$ 0.008
2.9-3.0	3217.4 $\pm$ 86.4	226.8 $\pm$ 20.7	-85.6 $\pm$ 313.5	22.3	-0.002 $\pm$ 0.008

TABLE II: Possible sources of systematic uncertainties in the inclusive  $\pi^0$  multiplicity measurement (results are preliminary).

Source	Effect on average $\pi^0$ multiplicity (%)
Overall normalization	1.6
$\Delta n = Y_{on} - \left(\frac{E_{on}}{E_{off}}\right) \left(\frac{s_{off}}{s_{on}}\right) \cdot Y_{off}$	2
OFF $E_{\gamma}^2 \cdot \sqrt{\left(\frac{s_{on}}{s_{off}}\right)}$	0.8
$E_{\gamma}$ non - linearity	0.6
Shower Shape	0.4
Track match	1.6
Fit procedure	3
Energy dependence of efficiency	0.3
Run dependence	4.6
Total	6.4